Quantum Electronics **49** (12) 1083–1088 (2019)

SPECIAL ISSUE DEVOTED TO THE 7TH ALL-RUSSIA CONFERENCE ON FIBER OPTICS https://doi.org/10.1070/QEL17172

Dynamics and quantum fluctuations of light in nonstationary operation modes of a Raman fibre amplifier

L.A. Mel'nikov, Yu.A. Mazhirina

Abstract. **We report the results of numerical simulation of the radiation dynamics in a Raman fibre amplifier taking into account quantum fluctuations of the pump fields and Stokes waves. The simulation relies on an approach based on solutions of the transport equations for complex amplitudes and on the 'backward' propagation method for operators describing quantum fluctuations. It is shown that there exists an optimal Raman amplifier length corresponding to the minimum level of fluctuations of the amplified Stokes pulse.**

Keywords: *stimulated Raman scattering, counterpropagating waves, transport equations, quantum fluctuations, perturbation method.*

1. Introduction

The dynamics of fibre lasers and amplifiers has been studied for a long time, and in many respects these investigations have been stimulated by new experimental results and possibilities provided by fibres and laser systems of new types. An important direction has always been the research of the dynamics of light in fibre lasers, where SRS or SBS pump conversion is used [1]. Unlike lasers based on activated fibres, lasing in Raman or SBS lasers is possible even in the absence of feedback in the cavity (single-pass lasing), because the SBS and SRS gain coefficients are large even at moderate pump powers, and fibre loss is negligible. The main dynamic phenomena in Raman or SBS fibre lasers with a linear asymmetric configuration (fibre is excited from one end face) are due to relaxation oscillations resulting from the action of a wave propagating towards the pump wave during SBS, or a Stokes wave copropagating with the pump wave during SRS [2–5]. Typically, these oscillations occur with a period equal to the round-trip time of light in the cavity, the length of which either coincides with the fibre length or is shorter due to the absorption of the pump. Then their period is determined by the time required for the light to pass a certain effective length [2]. In this case, the fibre dispersion is usually not taken into account, since the pulse durations are sufficiently long.

L.A. Mel'nikov, Yu.A. Mazhirina Yuri Gagarin State Technical University of Saratov, ul. Politekhnicheskaya 77, 410054 Saratov, Russia; Prokhorov General Physics Institute, Russian Academy of Sciences, ul. Vavilova 38, 119991 Moscow, Russia; e-mail: lam-pels@ya.ru

Received 24 October 2019
Kvantovaya Elektronika **49** (12) 1083–1088 (2019)
Translated by I.A. Ulitkin

Significantly, equations describing lasing are partial differential equations that cannot be reduced to a system of ordinary differential equations of small dimension. Therefore, analytical results can be obtained only with sufficiently rigid approximations that are often not justified in experiments [3]. For this reason, a numerical experiment plays an important role in the analysis of dynamic phenomena [1, 2, 5]. In the conventional approach, the equations are supplemented by boundary conditions at the end faces of fibre – the so-called two-point boundary-value problem, which is integrated using quite sophisticated methods. It often uses multiple runs along the fibre length to satisfy the boundary conditions. All these factors require time-consuming calculations and study of convergence of successive approximation procedures.

Raman lasers based on long (tens and hundreds of kilometres) fibres are used in telecommunication systems as distributed amplifiers [6]. Ring configurations of long fibre lasers are of particular interest, because optical gyroscopic devices can be designed on their basis. At the same time, a long fibre allows one to fabricate a cavity with a large scale factor that relates the phase incursion caused by rotation or the frequency difference of counterpropagating waves with the angular velocity of rotation [7]: $\Delta\omega = \Delta\nu 8\pi S/(c\lambda)$, where S is the area of the fibre contour; λ is the laser wavelength; $\Delta\nu = 2\pi v_g/L$ is the frequency spacing between the longitudinal modes of the ring cavity; L is the perimeter of the cavity; $v_g = (\mathrm{d}\beta/\mathrm{d}\omega)^{-1}$ is the group velocity; and β is the propagation constant at the laser frequency. It can be seen that at small group velocities the scale factor becomes very large [8].

In conventional ring lasers, due to the amplitude–phase lasing conditions, the linear coupling of counterpropagating waves leads to frequency locking at small differences in their frequencies, which prevents the measurement of low rotation velocities when the beat frequency is compared with the width of the lock-in zone. The width of this zone is estimated as Rc/L, where c/L is the mode spacing and R is the coupling coefficient of counterpropagating waves, which is 10^{-5}–10^{-6} in gas lasers. In optical fibres, due to Rayleigh scattering, this coefficient is $\sim 10^{-4}$ km^{-1}. However, as already noted, SRS lasing is not so sensitive to phase relations for the field in the cavity; therefore, one can hope to obtain information about the angular velocity of rotation even with such a large backscattering coefficient.

Recently, studies on the dynamics of light in long fibre lasers have been published, stimulated by the emergence of the concept of random feedback in optical fibre [9–12], when generation can occur almost in a single pass in the absence of mirrors under symmetric excitation of fibre [5, 13]. The role of Rayleigh scattering and spontaneous Raman scattering is to

produce seed fields for SRS, which makes it possible to develop various instabilities.

Many problems are related to the study of the dynamics of short light pulses in long fibre lasers. A number of papers have been recently published, where mode locking was obtained in a fibre laser using cavity elements with significantly different dispersion. This makes it possible to obtain regimes caused by instabilities resembling Faraday (parametric) instabilities [14, 15]. The propagation modes of short (picosecond) light pulses in fibres with dispersion periodically varying over length are also interesting for generating entangled soliton-like pulses [16]. It is known that the propagation of waves with constant intensity in optical fibres is accompanied by instability in the case of negative group-velocity dispersion [1]. However, similar instabilities are observed in the case of counterpropagating waves and cross-phase modulation even with a positive dispersion of the group velocity. Modulation of fibre dispersion parameters can also lead to parametric-type instability [5, 17].

To study the processes occurring in long fibre lasers and to construct adequate physical models of these processes, it is convenient to consider simplified configurations, which is done in this work. In addition, the numerical simulation relies on solving the transport equations for the field amplitudes of counterpropagating waves by applying grid methods and the Courant–Isaacson–Rees algorithm [18], which makes it possible to study the laser dynamics for a large number of passes through fibre without using iterative algorithms [5, 13].

2. Quantum equations for a Raman fibre amplifier

2.1. Equations for fields

We will use the expansion of the fields in travelling waves:

$$\begin{aligned} \boldsymbol{E}_X(x,y,z,t) &= \frac{1}{2}\boldsymbol{e}\psi(x,y)\exp(\mathrm{i}\beta_0 z - \mathrm{i}\omega_0 t)\mathcal{E}_X(z,t) + \text{c. c.},\\ \mathcal{E}_X(z,t) &= \exp[\mathrm{i}\beta_0 z - \mathrm{i}\omega(\beta_0)t]\\ &\quad\times\sum_{k=-\infty}^{\infty} X_k \exp[\mathrm{i}(\beta_k-\beta_0)z - \mathrm{i}(\omega_k-\omega_0)t]\\ &= \int_{-\infty}^{\infty}\frac{\mathrm{d}\eta}{2\pi}X(\eta)\exp\{\mathrm{i}(\eta-\beta_0)z - \mathrm{i}[\omega(\eta+\beta_0)-\omega_0]t\}. \end{aligned} \tag{1}$$

Here, $\boldsymbol{e}$ is the unit vector of wave polarisation; $\psi(x,y)$ is the mode function [19]; β is the propagation constant of the fundamental mode; $\omega_0 = \omega(\beta_0)$ is the frequency of the carrier field at $\beta = \beta_0$; $\beta_k = \beta_0 + 2\pi v_X k/L$; v_X is the phase velocity; L is the fibre length; $\eta = \beta - \beta_0$; $X(\eta)$ is the Fourier amplitude of the spatial spectrum; $X = F, B, F_\mathrm{s}, B_\mathrm{s}$; F and B are the amplitudes of the pump waves (the amplitude F corresponds to the waves propagating along the z axis, and the amplitude B corresponds to counterpropagating waves); and F_s and B_s are the amplitudes of the Stokes waves. For long fibres, integration is used instead of summation. After replacing the classical field with a quantised one and normalising the amplitudes to the field corresponding to one quantum in the volume V that it occupies [20], we obtain

$$\hat{\mathcal{E}}_X(z,t) = \sqrt{\frac{\hbar\omega_0}{\varepsilon_0\varepsilon V}}\left[\hat{X}(z,t) + \hat{X}^\dagger(z,t)\right],$$

where $\hat{X}(z,t)$ and $\hat{X}^\dagger(z,t)$ are field annihilation and creation operators, which, due to expressions (1), are a superposition of the creation and annihilation operators of individual longitudinal modes (travelling waves); and ε and ε_0 are the permittivities of the fibre and vacuum, respectively. For these operators, the ordinary commutation relations

$$[\hat{X}(z,t)\hat{X}^\dagger(z',t')] = \delta(t-t')\delta(z-z')$$

are satisfied.

The equations for the operators of the fields of Stokes and pump waves at sufficiently long pulses, for which the dispersion can be ignored, are taken from [13] with the corresponding replacement of the amplitudes of the envelope fields with the operators:

$$\frac{\partial\hat{F}}{\partial t} + v_\mathrm{g}\frac{\partial\hat{F}}{\partial z} = -g(\hat{F}_\mathrm{s}^\dagger\hat{F}_\mathrm{s} + \hat{B}_\mathrm{s}^\dagger\hat{B}_\mathrm{s})\hat{F} - \gamma F + \hat{N}_F, \tag{2}$$

$$\frac{\partial\hat{B}}{\partial t} - v_\mathrm{g}\frac{\partial\hat{B}}{\partial z} = -g(\hat{F}_\mathrm{s}^\dagger\hat{F}_\mathrm{s} + \hat{B}_\mathrm{s}^\dagger\hat{B}_\mathrm{s})\hat{B} - \gamma B + \hat{N}_B, \tag{3}$$

$$\frac{\partial\hat{F}_\mathrm{s}}{\partial t} + v_\mathrm{gs}\frac{\partial\hat{F}_\mathrm{s}}{\partial z} = g_\mathrm{s}(\hat{F}_\mathrm{s}^\dagger\hat{F} + \hat{B}^\dagger\hat{B})\hat{F}_\mathrm{s} - \gamma_\mathrm{s}\hat{F} + \hat{N}_{F_\mathrm{s}}, \tag{4}$$

$$\frac{\partial\hat{B}_\mathrm{s}}{\partial t} + v_\mathrm{gs}\frac{\partial\hat{B}_\mathrm{s}}{\partial z} = g_\mathrm{s}(\hat{F}^\dagger\hat{F} + \hat{B}^\dagger\hat{B})\hat{B}_\mathrm{s} - \gamma_\mathrm{s}\hat{B} + \hat{N}_{B_\mathrm{s}}, \tag{5}$$

where g_s is the gain of the Stokes waves; $g = g_\mathrm{s}\omega_\mathrm{p}/\omega_\mathrm{s}$; ω_p and ω_s are the frequencies of the pump wave and the Stokes wave; γ and γ_s are the loss coefficients at the frequencies of the pump wave and the Stokes wave; v_g and v_gs are the group velocities of the pump wave and the Stokes wave; $\hat{N}_X$ are the sources of fluctuations cause by medium losses, mirror losses and Raman gain.

2.2. Backpropagation method

The solution of the system of equations (2)–(5) for field operators is a rather difficult task, because the dimension of the space in which the operator acts is very large and is determined by the number of longitudinal modes and the number of quanta in each mode. There is a method based on the representation of field operators as the sum of the 'classical' and quantum parts, with the quantum part being treated as a small perturbation [21]. This method has been successfully used to study quantum fluctuations during the propagation of optical solitons [22–24] and to solve similar problems, which are reduced to analysis of the propagation of short light pulses in nonlinear media with Kerr nonlinearity, dispersion, amplification and loss [25, 26]. A characteristic feature of these problems is the propagation of pulses (one or several) in one direction. This allows one to introduce a coordinate system synchronised with the pulse propagation ($z, t - z/v_\mathrm{g}$) and use the z coordinate as an evolutionary variable. Because standing waves (or a pair of counterpropagating travelling waves coupled through reflections on mirrors) serve as longitudinal eigenmodes in a fibre laser with mirrors at the end faces, it is convenient to choose time t as an evolutionary variable. Moreover, derivatives with respect to z are not excluded when replacing time t with the current pulse time,

and the boundary conditions are also significant. An additional complication is the presence of four coupled waves whose quantum operators act on different state vectors. Therefore, the backpropagation scheme must be modified accordingly.

According to the results of Refs [21, 24], it is necessary to distinguish in each field operator $\hat{X}(z,t)$ the classical field $X(z,t)$ and the perturbation operator $\hat{u}_X(z,t)$: $\hat{X} = X + \hat{u}_X(z,t)$; moreover, all quantum properties are described by $\hat{u}_X$. Under the condition of small perturbations, $\int \mathrm{d}z X^* X \gg \langle | \hat{u}_X^\dagger \hat{u}_X | \rangle$, we can go over to the equations for perturbations $\hat{f}, \hat{b}, \hat{f}_\mathrm{s}, \hat{b}_\mathrm{s}$, in which $\hat{X}$ should be replaced by classical fields X. These classical fields obey equations (2)–(5), where operator symbols are removed and there are no noise sources. Boundary conditions can be written separately for linear and ring cavities.

2.3. Linear cavity

We assume that a fibre segment of length L is excited on the left and on the right and that the waves (Stokes) can be reflected on the right and left ends. Then,

$$F_\mathrm{s}(0,t) = \sqrt{R_\mathrm{left}}\, B_\mathrm{s}(0,t), \quad B_\mathrm{s}(L,t) = \sqrt{R_\mathrm{right}}\, F_\mathrm{s}(L,t), \tag{6}$$

$$\begin{aligned} F(0,t) &= \sqrt{R_\mathrm{left}}\, B(0,t) + \sqrt{W_\mathrm{left}(t)}\,, \\ B(L,t) &= \sqrt{R_\mathrm{right}}\, F(L,t) + \sqrt{W_\mathrm{right}(t)}\,. \end{aligned} \tag{7}$$

Here, R_left and R_right are power reflectances on the left and right ends of fibre, respectively; W_left and W_right are the pump powers; and β and β_s are the propagation constants for pump waves and Stokes waves.

2.4. Ring cavity

We assume that a fibre segment of length L is rolled into a ring and is excited through a WDM coupler by waves propagating clockwise (wave F) and counterclockwise (wave B) in the ring. We also assume that the coupler is not ideal, which leads to coupling of counterpropagating Stokes waves, and there are no reflections at the pump frequency. Then,

$$\begin{aligned} F_\mathrm{s}(0,t) &= \sqrt{R}\, B_\mathrm{s}(0,t) + \sqrt{1-R}\, F_\mathrm{s}(L,t), \\ B_\mathrm{s}(L,t) &= -\sqrt{R}\, F_\mathrm{s}(L,t) + \sqrt{1-R}\, B_\mathrm{s}(0,t), \end{aligned} \tag{8}$$

$$F(0,t) = F(L,t) + \sqrt{W_\mathrm{left}(t)}, \quad B(L,t) = B(0,t) + \sqrt{W_\mathrm{right}(t)}\,.$$

For the operators $\hat{f}, \hat{b}, \hat{f}_\mathrm{s}, \hat{b}_\mathrm{s}$, the boundary conditions are the same. For these operators we obtain linear equations that can be written in compact form:

$$\frac{\partial \hat{u}}{\partial t} = \hat{P}\hat{u} + \hat{Q}\hat{u}^\dagger + \hat{N}, \tag{9}$$

where

$$\hat{u} = \begin{pmatrix} \hat{f} \\ \hat{b} \\ \hat{f}_\mathrm{s} \\ \hat{b}_\mathrm{s} \end{pmatrix}; \quad P_\mathrm{s} = |F_\mathrm{s}|^2 + |B_\mathrm{s}|^2, \quad P = |F|^2 + |B|^2; \quad \hat{P} =$$

$$\begin{pmatrix} -v_\mathrm{g}\frac{\partial}{\partial z} - \gamma - gP_\mathrm{s} & 0 & -gFF_\mathrm{s}^* & -g_\mathrm{s}FB_\mathrm{s}^* \\ 0 & v_\mathrm{g}\frac{\partial}{\partial z} - \gamma - gP_\mathrm{s} & -gBF_\mathrm{s}^* & -g_\mathrm{s}BB_\mathrm{s}^* \\ g_\mathrm{s}F^*F_\mathrm{s} & gB^*F_\mathrm{s} & -v_{\mathrm{gs}}\frac{\partial}{\partial z} - \gamma_\mathrm{s} + gP & 0 \\ g_\mathrm{s}F^*B_\mathrm{s} & gB^*B_\mathrm{s} & 0 & v_{\mathrm{gs}}\frac{\partial}{\partial z} - \gamma_\mathrm{s} + gP \end{pmatrix};$$

$$\hat{Q} = \begin{pmatrix} 0 & 0 & -gFF_\mathrm{s} & -g_\mathrm{s}FB_\mathrm{s} \\ 0 & 0 & -gBF_\mathrm{s} & -g_\mathrm{s}BB_\mathrm{s} \\ gFF_\mathrm{s} & g_\mathrm{s}BF_\mathrm{s} & 0 & 0 \\ gFB_\mathrm{s} & g_\mathrm{s}BB_\mathrm{s} & 0 & 0 \end{pmatrix}; \quad \hat{N} = \begin{pmatrix} \hat{N}_F \\ \hat{N}_B \\ \hat{N}_{F_\mathrm{s}} \\ \hat{N}_{B_\mathrm{s}} \end{pmatrix}.$$

Note that due to the boundary conditions between the operators $\hat{f}, \hat{b}$ and $\hat{f}_\mathrm{s}, \hat{b}_\mathrm{s}$ there is a linear coupling. The matrix $\hat{P}$ is anti-Hermitian, and the matrix $\hat{Q}$ is antisymmetric.

To fulfil the standard commutation relations for operators, it is necessary, as usual [20, 21], to introduce a restriction on noise sources. Following [21], we easily obtain expressions

$$\begin{aligned} &\left[\hat{N}_X(t,z_1), \hat{N}_Y^\dagger(t',z_2)\right] = M_X(t,z_1,z_2)\delta(t-t')\delta_{XY}\,, \\ &\left[\hat{N}_X(t,z_1), \hat{N}_X(t',z_2)\right] = \left[\hat{N}_X^\dagger(t,z_1), \hat{N}_X^\dagger(t',z_2)\right] = 0\,, \\ &\left[\hat{N}_X(t,z_1), \hat{N}_Y(t',z_2)\right] = \left[\hat{N}_X^\dagger(t,z_1), \hat{N}_Y^\dagger(t',z_2)\right] = 0\,, \\ &M_X(t,z_1,z_2) = -\left[\hat{P}(t,z_1) - \hat{P}^*(t,z_2)\right]_{XX}\delta(z_1 - z_2)\,, \\ &X, Y = F, B, F_\mathrm{s}, B_\mathrm{s}\,. \end{aligned} \tag{10}$$

In addition to commutators, to calculate quantum fluctuations, one needs to know the correlation functions

$$\langle \hat{N}_X(t_1,z_1)\hat{N}_Y^\dagger(t_2,z_2)\rangle, \ \langle \hat{N}_X(t_1,z_1)\hat{N}_Y(t_2,z_2)\rangle\,,$$

$$\langle \hat{N}_X^\dagger(t_1,z_1)\hat{N}_Y(t_2,z_2)\rangle, \ \langle \hat{N}_X^\dagger(t_1,z_1)\hat{N}_Y^\dagger(t_2,z_2)\rangle\,,$$

which can be determined if there is information about the physical nature of noises in the problem in question. For example, noise sources were calculated for intrapulse SRS in [21].

Quantum-mechanical average values measured at time $t = T$ can be tied to a specific point of fibre or averaged over its entire length or over a selected segment. In these cases, it will be necessary to calculate scalar products of the form

$$\{\mathcal{F}|u_X\} = \frac{1}{2}\int_0^L \mathrm{d}z\left[\mathcal{F}^*(z,T)\hat{u}_X(z,T) + \mathcal{F}(z,T)\hat{u}_X^\dagger(z,T)\right], \tag{11}$$

where $\mathcal{F}(z,T)$ characterises spatial filtering during the measurement, and it is assumed that this function is normalised. For example, the operator X of the number of quanta in the wave has the form

$$\hat{X}^\dagger\hat{X} = X(z,T)X^*(z,T) + [X(z,T)\hat{u}_X^\dagger(z,T) + \text{h.c.}].$$

It follows that we need to set $\mathcal{F}(z,T) = X(z,T)$.

To perform quantum-mechanical averaging, we will use coherent states corresponding to the classical states $X(z,t)$ shifted by the amplitude of the classical field [24]. Thus, we obtain a multimode vacuum state $|0_X\rangle$, for which

$\langle 0_X | \hat{u}_X(z,t) | 0_X \rangle = 0$. At the same time, the quantum-mechanical average value of the field is equal to its classical part, and the average number of quanta is

$$\langle n_X \rangle = \int_0^L \mathrm{d}z \, | X(z,t) |^2 .$$

To significantly simplify the calculations of integrals of form (11), we can introduce an adjoint operator [21, 27] using the definition

$$\{\tilde{F} | \hat{P}\hat{u}\} + \{\tilde{F} | \hat{Q}\hat{u}^{\dagger}\} = \{\hat{P}^{\mathrm{A}}\tilde{F} | \hat{u}\} + \{\hat{Q}^{A}\tilde{F} | \hat{u}^{\dagger}\},$$

where $\tilde{F}$ is the diagonal matrix with main diagonal elements $\mathcal{F}_f, \mathcal{F}_b, \mathcal{F}_{f_s}, \mathcal{F}_{b_s}$. Then, instead of solving the operator equation (9) with a stochastic source, it is necessary to solve the equation for the matrix $\tilde{F}$:

$$\frac{\partial F}{\partial t} = \hat{P}^{\mathrm{A}}\tilde{F} + \hat{Q}^{\mathrm{A}}\tilde{F}^{*}. \tag{12}$$

Moreover, the initial condition for it is given at $t = T$, but its values should be known starting from $t = 0$, because they are needed to calculate quantum corrections. Therefore, this equation must be solved in the opposite direction along t. To find expressions for the adjoint operator, one can use integration by parts. It is easy to obtain that $\hat{P}^{\mathrm{A}} = \hat{P}$ with a simultaneous replacement of the signs of the derivatives with respect to z and $\hat{Q}^{\mathrm{A}} = -\hat{Q}$, and moreover, one must choose $\mathcal{F}_X(0,T) = \mathcal{F}_X(L,T) = 0$. Due to a certain arbitrary choice of functions, this is not difficult to do. With this choice of the adjoint operator, if F satisfies equation (12), the condition

$$\frac{\partial}{\partial t}\{\tilde{F}(z,t)\tilde{u}(z,t)\} = 0$$

is met. It yields the expression for the measured averages:

$$\frac{\partial}{\partial t}\{\mathcal{F}_X | \hat{u}_X\} = \{\mathcal{F}_X | \hat{N}_X\}. \tag{13}$$

This gives the relation

$$\{\mathcal{F}_X(z,T) | \hat{u}_X(z,T)\} = \{\mathcal{F}_X(z,0) | \hat{u}_X(z,0)\} + \int_0^T \mathrm{d}t \, \{\mathcal{F}_X(z,t) | \hat{N}_X(z,t)\}. \tag{14}$$

Using (13) and (14), one can obtain all the expressions necessary for calculating quantum fluctuations, similar to those obtained in [21]:

$$\langle \Delta n_X^2 \rangle |_{t=T} = \langle \Delta n_X^2(z,0) \rangle |_{t=0} + \frac{1}{4}\int_0^T \int_0^T \int_0^L \int_0^L \mathrm{d}t_1 \, \mathrm{d}t_2 \, \mathrm{d}z_1 \, \mathrm{d}z_2 \times [\mathcal{F}_{1X}^{*}\mathcal{F}_{2X}^{*} \langle N_{1X}N_{2X} \rangle + \mathcal{F}_{1X}\mathcal{F}_{2X}^{*} \langle N_{1X}^{\dagger}N_{2X} \rangle] + \mathrm{h.c.} \tag{15}$$

Here, the subscripts 1 and 2 in the integrand indicate the arguments z_1, t_1 and z_2, t_2, and the expressions for $\mathcal{F}$ correspond to normalised classical field amplitudes. For example,

$$\mathcal{F}_f(z,T) = \frac{F(z,T)}{\sqrt{\int \mathrm{d}z \, | F(z,T) |^2}}.$$

3. Integration method

In the general case, there are no analytical solutions to the equations for classical fields; therefore, numerical simulation was used in the work to calculate both the classical part of the field and quantum uncertainties (15). In the calculations, it is convenient to use the normalised coordinates $Z = z/L$ and $T = tv_g/L$, as well as to normalise the amplitudes by $\sqrt{W}$. Then, the equations contain dimensionless linear gain and absorptions: $gL, \gamma L$ and $\gamma_s L$.

Equations (2)–(5) are the transport equations $(\partial/\partial t \pm \partial/\partial z) U(z,t) = V(z,t)$ (the '+' sign refers to the wave propagating in the positive direction, the '–' sign refers to the wave propagating in the negative direction)], which are conveniently integrated numerically using the Courant–Isaacson–Rees scheme [18]:

$$U(z,t) \to U(z_m,t_n) = U_{mn},$$

$$z_m - z_{m-1} = \mathrm{d}z, \quad t_n - t_{n-1} = \mathrm{d}t, \quad \sigma = \mathrm{d}t/\mathrm{d}z, \quad \sigma \le 1,$$

$$U_{m\,n+1} = (1-\sigma)\,U_{mn} + \sigma U_{m\pm 1\,n} + V_{mn}\mathrm{d}t.$$

4. Results of calculations

In the calculations, we used the following parameters: $g_s = 0.6\ \mathrm{km^{-1}\,W^{-1}}$, $\gamma = 0.055\ \mathrm{km^{-1}}$, $\gamma_s = 0.046\ \mathrm{km^{-1}}$, $L = 22.5$ km [13]. With such a fibre length and moderate pump intensities not exceeding the threshold for the appearance of second-order Stokes waves, the $g_s P/\gamma$ values of about 100 can be achieved. Regimes in which pump radiation is almost completely absorbed in fibre can also be obtained and, in addition, the specified fibre length corresponds to that used in the experiment [13]. At shorter fibre lengths, the appearance of relaxation oscillations [2] requires higher pump intensities. At larger fibre lengths, the observed regimes are qualitatively similar to those at $L = 22.5$ km. Because spontaneous Raman scattering is significant only in regions where the Stokes wave intensities are small (i.e., at the ends of fibre), its contribution was modelled by illumination (with a power of 10^{-5} W) of the corresponding end faces: the left and right end faces of fibre were illuminated for the F wave and the B wave, respectively. It was verified that variations in the illumination power do not affect the system dynamics. It was also found that scattering of $\sim 10^{-4}\ \mathrm{km^{-1}}$ does not significantly affect the dynamics and the impact of scattering is similar to that of illumination. Therefore, scattering was not taken into account. At the same time, the presence of reflections at the end faces of fibre is essential for the dynamics. First, if the pump is not completely absorbed along the length of fibre, then there appear a reflected pump wave and a corresponding gain in the counterpropagating wave. Secondly, the intensity of the Stokes wave reflected from the end face can exceed the illumination intensity, which is significant for the development of relaxation oscillations.

It was assumed that the pump field instantly turns on at $t = 0$. A pump wave propagates along the z axis. At the same time, a continuously amplified Stokes wave copropagates with the pump wave. A counterpropagating Stokes wave is generated in the regions reached by the pump wave. Both Stokes waves deplete the pump wave. The transient process continues for ~ 10 passes through the fibre.

Because the characteristic times and spatial scales of the field changes in long fibres (on the order of 1 km or more) pumped by the light with a constant intensity at the fibre input lie in the ranges of microseconds and hundreds of meters, dispersion can be neglected.

4.1. Special case. Raman amplifier

Let us consider a simplified situation when a pump pulse and a pulse at the Stokes frequency are launched into a fibre of length L. In this case, there are no reflections at the boundaries, and the boundary conditions are as follows:

$$F(0,t) = \sqrt{W(t)}, \quad F_{\rm s}(0,t) = \sqrt{W_{\rm s}(t)}\,.$$

The equations for classical fields can be represented as

$$\begin{aligned} &\frac{\partial F}{\partial t} + v_{\rm g}\frac{\partial F}{\partial z} = -\gamma F - g_{\rm s}|F_{\rm s}|^2 F\,,\\ &\frac{\partial F_{\rm s}}{\partial t} + v_{\rm gs}\frac{\partial F_{\rm s}}{\partial z} = -\gamma_{\rm s}\hat{F} + g|F|^2 F_{\rm s}, \end{aligned} \tag{16}$$

the equations for $\hat{f}$ and $\hat{f}_{\rm s}$ have the form

$$\begin{aligned} &\frac{\partial \hat{f}}{\partial t} = -v_g\frac{\partial \hat{f}}{\partial z} - \gamma\hat{f} - g_{\rm s}|F_{\rm s}|^2\hat{f} - g_{\rm s}FF_{\rm s}^*\hat{f}_{\rm s} - g_{\rm s}FF_{\rm s}\hat{f}_{\rm s}^\dagger,\\ &\frac{\partial \hat{f}_{\rm s}}{\partial t} = -v_{\rm gs}\frac{\partial \hat{f}_s}{\partial z} - \gamma\hat{f}_{\rm s} + g|F|^2\hat{f}_{\rm s} - gF_{\rm s}F^*\hat{f} + gF_{\rm s}F\hat{f}^\dagger, \end{aligned} \tag{17}$$

and the equations for $\mathcal{F}_f$ and $\mathcal{F}_{f_{\rm s}}$ have the form

$$\begin{aligned} &\frac{\partial \mathcal{F}_f}{\partial t} = v_{\rm g}\frac{\partial \mathcal{F}_f}{\partial z} - \gamma\mathcal{F}_f - g_{\rm s}|F_{\rm s}|^2\mathcal{F}_f - g_{\rm s}FF_{\rm s}^*\mathcal{F}_{f_{\rm s}} + g_{\rm s}FF_s\mathcal{F}_{f_{\rm s}}^*\,,\\ &\frac{\partial \mathcal{F}_{f_{\rm s}}}{\partial t} = v_{\rm gs}\frac{\partial \mathcal{F}_{f_{\rm s}}}{\partial z} - \gamma\mathcal{F}_{f_{\rm s}} + g|F|^2\mathcal{F}_{f_{\rm s}} + gF_{\rm s}F^*\mathcal{F}_f - gF_{\rm s}F\mathcal{F}_{f_{\rm s}}^*\,. \end{aligned} \tag{18}$$

As the initial conditions for (18), we choose the conditions $\mathcal{F}_f(z,T) = F(z,T)$, $\mathcal{F}_{f_{\rm s}} = F_{\rm s}(z,T)$ and numerically determine the dependences $\mathcal{F}_f(z,t)$ and $\mathcal{F}_{f_{\rm s}}(z,t)$.

Figure 1 shows the spatiotemporal dependences of the intensities of the pump wave and the Stokes wave, as well as the functions $|\mathcal{F}_f(z/L, t/\tau)|^2$ and $|\mathcal{F}_{f_{\rm s}}(z/L, t/\tau)|^2$, where τ is the duration of the pump pulse. One can see that the appearance of the Stokes pulse leads to depletion of the pump, which is manifested in the occurrence of a dip at the tail of the pump pulse.

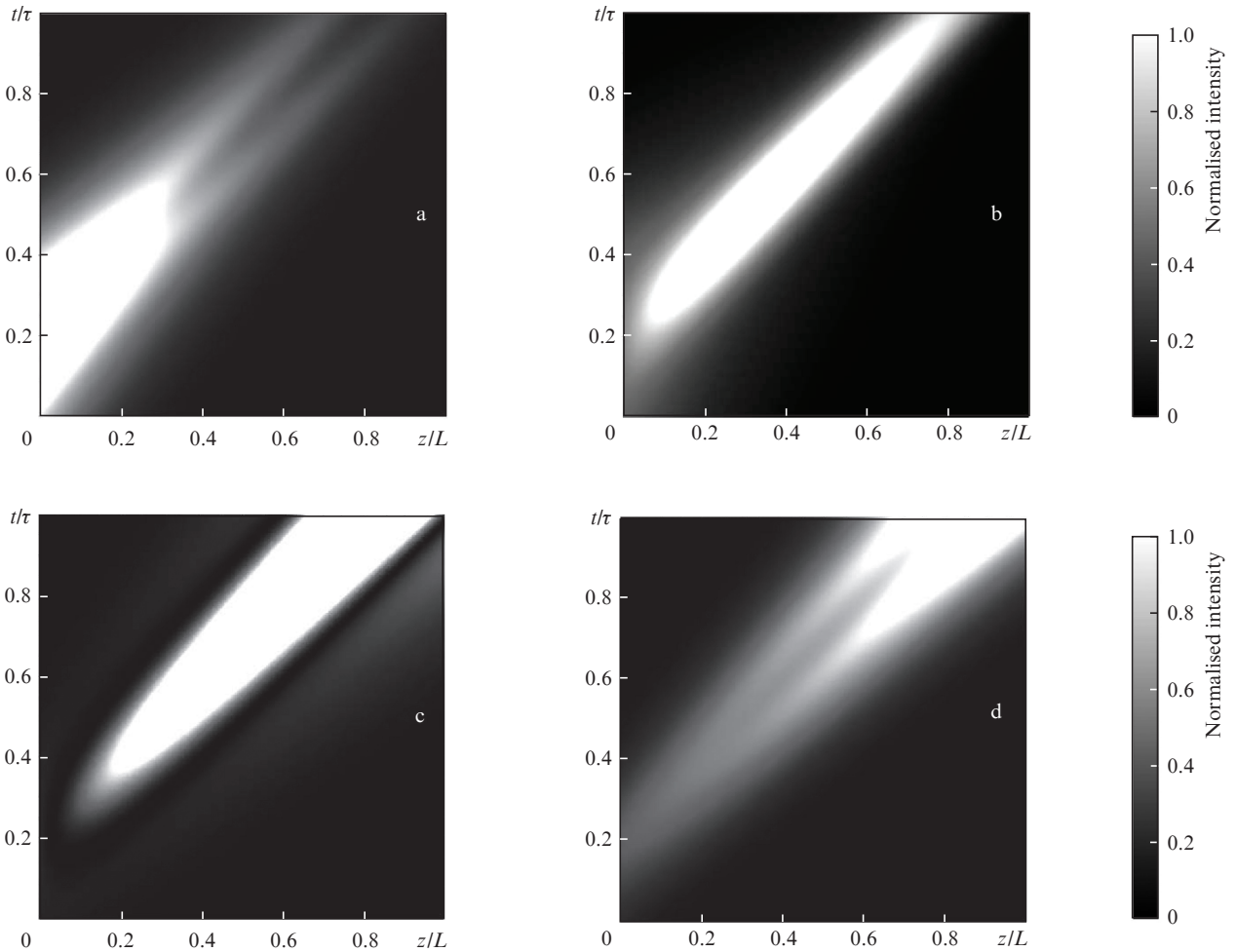

Figure 1. (a) Pump wave and (b) Stokes wave intensities of the, as well as (c) $|\mathcal{F}_f(z/L, t/\tau)|^2$ and (d) $|\mathcal{F}_{f_{\rm s}}(z/L, t/\tau)|^2$ functions vs. time and coordinate at $g = 0.6$ km^{-1} W^{-1}, $g_{\rm s} = 0.553$ km^{-1} W^{-1}, normalised pump wave and Stokes wave powers $W(t/\tau) = \mathrm{sech}(t/\tau)$ and $W_{\rm s}(t/\tau) = 0.1\mathrm{sech}(t/\tau)$, $\gamma = 0.055$ km^{-1}, $\gamma_{\rm s} = 0.046$ km^{-1} and $L = 22.5$ km.

Figure 2 shows the time dependences of the level of quantum fluctuations of the pump wave and the Stokes wave with respect to the initial level of fluctuations at the input to the fibre under the assumption that the fields at the input are in a coherent state. One can see that at distances corresponding to a transit time of 0.2τ, the Stokes wave has a level of quantum fluctuations of about 3 dB less than at the input. With a further increase in transit time, the level of fluctuations is restored and continues to grow, reaching a level 3 dB higher than the level of initial fluctuations, at a distance corresponding to a transit time of 0.35τ. This means that there exists an optimal length of the Raman amplifier. The appearance of a minimum level of quantum fluctuations can be explained by the fact that the noise level increases in proportion to the number of photons. Relative fluctuations decrease with increasing number of photons; therefore, when the pump is depleted, the level of quantum fluctuations increases, which is shown in Fig. 2. With an increase in the number of photons in the Stokes wave, the relative fluctuations of the number of quanta decrease and then begin to increase due to an increase in the level of fluctuations of the pump wave. These results are in qualitative agreement with the results of [28], in which quantum fluctuations were calculated by other methods.

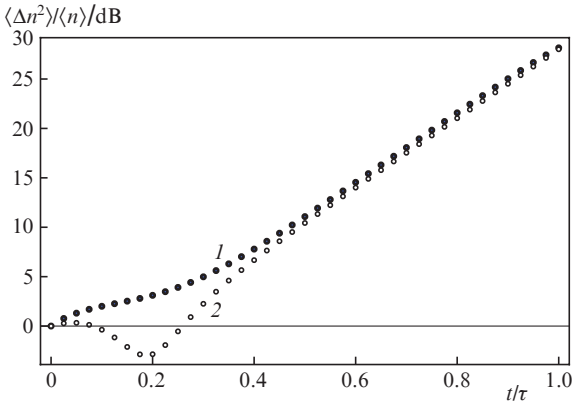

Figure 2. Time dependences of the level of fluctuations $\langle \Delta n^2 \rangle / \langle n \rangle$ of (*1*) pump and (*2*) Stokes waves.

5. Conclusions

We have presented the results of numerical simulation of the nonlinear dynamics of the light in Raman fiber lasers and distinctive features of the manifestation of instabilities of Raman lasing. The use of techniques used in the theory of transfer in numerical simulation has made it possible to propose and implement an effective numerical algorithm that allows one to trace the dynamics of a laser system at large times, corresponding to tens and hundreds of thousands of passes through the cavity.

Acknowledgements. The part of the work concerning the use of long Raman lasers was supported in part by the Ministry of Education and Science of the Russian Federation (Project No. 9.2108.2017/PCh). The part dealing with quantum fluctuations in Raman amplifiers/Raman lasers was supported by the Russian Science Foundation (Project No. 17-12-01564).

References

1. Agraval G.P. *Nonliner Fiber Optics* (Waltham: Academic Press, 2013).
2. Jhonson R.V., Marburger J.H. *Phys. Rev. A*, **4**, 1175 (1971).
3. Bar-Joseph I. *J. Opt. Soc. Am. B*, **2**, 1606 (1985).
4. Narum P. *J. Opt. Soc. Am. B*, **5**, 623 (1988).
5. Mel'nikov L.A., Mazhirina Yu.A. *Quantum Electron*., **47**, 1083 (2017) [*Kvantovaya Elektron*., **47**, 1083 (2017)].
6. Ania-Castañón J.D. et al. *Phys. Rev. Lett*., **101**, 123903 (2008).
7. Melnikov L.A. et al. *Proc. Symposium Gyro Technology* (Karlsruhe, Germany, 2011) Vol. 8, p.7.
8. Desurvire E., Kim B., Fesler K., Shaw H. *J. Lightwave Technol.*, **47**, 481 (1988).
9. Churkin D.V. et al. *Nat. Commun*., **6**, 6214 (2015).
10. Churkin D.V. et al. *Nat. Commun*., **6**, 7004 (2015).
11. Turitsyna E.G. et al. *Nat. Photonics*, **7**, 783 (2013).
12. Aragoneses A. et al. *Phys. Rev. Lett.*, **116**, 033902 (2016).
13. Mazhirina Yu.A. et al. *Izv. Vyssh. Uchebn. Zaved., Ser. Prikl. Nelin. Dinam*., **22**, 73 (2014).
14. Perego A.M. et al. *Phys. Rev. Lett.*, **116**, 028701 (2016).
15. Tarasov N. et al. *Nat. Commun*.,**7**, 12441 (2016).
16. Konukhov A.I. et al. *Laser Phys*., **12**, 055103 (2015).
17. Conforti M. el al. *Phys. Rev. Lett*., **116**, 028701 (2016).
18. Courant R., Isaacson E., Rees M. *Commun. Pure Appl. Math*., **5**, 243 (1952).
19. Love J., Snyder A. *Optical Waveguide Theory* (New York: Chapman and Hall, 1983; Moscow: Radio i Svyaz', 1987).
20. Scully M.O., Sargent M. III, Lamb W.E. *Laser Physics* (Deading, Mass.: Addison-Wesley, 1974).
21. Lai Y., Yu S.-S. *Phys. Rev. A*, **51**, 817 (1995).
22. Lai Y., Haus H.A. *Phys. Rev. A*, **40**, 844 (1989).
23. Mecozzi A., Kumar P. *Opt. Lett.*, **22** (16), 1232 (1997).
24. Matsko A.B., Kozlov V.V. *Phys. Rev. A*, **62**, 033811 (2000).
25. Lee R.-K., Lai Y., Malomed B.A. *Phys. Rev. A*, **70** (6), 063817 (2004).
26. Lee R.-K., Lai Y., Malomed B.A. *Phys. Rev. A*, **71** (1), 013816 (2005).
27. Haus H., Islam M. *IEEE J. Quantum Electron.*, **21** (8), 1172 (1985).
28. Miranowicz A., Kielich A., in *Advances in Chemical Physics* (New York: Wiley, 1994) Vol. 85 (III), pp 531 – 626.